



Simulation of roller compaction using a laboratory scale compaction simulator

Andrey V. Zinchuk*, Matthew P. Mullarney, Bruno C. Hancock

Global Research and Development, Pharmaceutical Research and Development, Pfizer Inc., MS-8156-007, Eastern Point Road, Groton, CT 06340, USA

Received 2 July 2003; received in revised form 23 September 2003; accepted 23 September 2003

Abstract

A method for simulation of the roller compaction process using a laboratory scale compaction simulator was developed. The simulation was evaluated using microcrystalline cellulose as model material and ribbon solid fraction and tensile strength as key ribbon properties. When compacted to the same solid fractions, real and simulated ribbons exhibited similar compression behavior and equivalent mechanical properties (tensile strengths). Thus, simulated and real ribbons are expected to result in equivalent granulations. Although the simulation cannot account for some roller compaction aspects (non-homogeneous ribbon density and material bypass) it enables prediction of the effects that critical parameters such as roll speed, pressure and radius have on the properties of ribbons using a fraction of material required by conventional roller compaction equipment. Furthermore, constant ribbon solid fraction and/or tensile strength may be utilized as scale up and transfer factors for the roller compaction process. The improved material efficiency and product transfer methods could enable formulation of tablet dosage forms earlier in drug product development.

© 2003 Elsevier B.V. All rights reserved.

Keywords: Roller compaction; Simulation; Microcrystalline cellulose; Solid fraction; Tensile strength

1. Introduction

Roller compaction is commonly used to increase material density, improve flow and help ensure final blend uniformity without application of heat or moisture to the materials (Sheskey et al., 1994; Miller, 1997; Adeyeye, 2000). Despite the widespread use of roller compaction, the current techniques for successful implementation of this unit operation still rely on material- and time-intensive procedures. For instance, feasibility of roller compaction as a processing option

is usually established using conventional scale equipment and thus may be difficult to accomplish early in the formulation development process when only small amounts drug substance are available. This concern has been recognized and recent investigations aiming to address this issue have been reported (Gereg and Cappola, 2002). These studies utilized a tablet press for production of the tablet-shaped, surrogate ribbons, which were subsequently used in milling and tableting evaluations. These assessments, however, did not address the unique characteristics of roller compaction such as roller compaction specific compression events and ribbon mechanical properties.

Similar to establishment of roller compaction feasibility, current approaches to scale-up of this process require significant amounts of material for

* Corresponding author. Tel.: +1-860-715-4805; fax: +1-860-441-3972.

E-mail address: andrey_v_zinchuk@groton.pfizer.com (A.V. Zinchuk).

experimentation. The scale-up also depends on the use of equipment parameters such as gauge pressure or force, which are prone to bias through equipment type and instrumentation. For example, accurate roll pressure scaling necessitates the measurement of maximum compression force exerted by the compactor to be transformed to compression pressure distribution. This transformation requires the prior knowledge of powder flow behavior (angles of internal and roll surface friction), predetermined material compressibility and several key assumptions regarding the friction and flow behavior of the material (Johanson, 1965, 1973). Even when compaction pressure distributions are known, conclusions regarding ribbon equivalency during scaling cannot be made until the ribbons are manufactured on a conventional roller compactor. This is due to the fact that the outcome of roller compaction is determined based on the characterization of granule or tablet properties (Falzone et al., 1992; Inghelbrecht and Remon, 1998; Murray et al., 1998; Adeyeye, 2000). Characterization of ribbons, the direct products of roller compaction, is commonly limited to the measurement of ribbon thickness, as well as subjective and qualitative strength tests.

For other unit operations such as tableting and capsule filling, the need for material sparing feasibility assessment and identification of scale-up specific process and product parameters has been addressed by development of bench scale simulations. Unique sim-

ulators for tableting and capsule filling instruments have been designed and have facilitated improved development and fundamental research in these areas (Jolliffe et al., 1982; Celik and Marshall, 1989; Bateman et al., 1989; Britten et al., 1996; Heda et al., 1999). For roller compaction however, no such bench scale simulations have been reported in the literature or are available commercially.

The aim of this publication is to address some of the challenges of the current state of roller compaction. The work reported herein presents a method for simulation of the roller compaction process along with the techniques for quantitative evaluation of its products. It includes three major components: a simulation of the compression events occurring during roller compaction using a compaction simulator, an illustration of how material relative density (solid fraction) can be used to characterize powders at different stages of densification and the use of solid fraction and tensile strength for the evaluation of equivalency between “simulated” and real roller compaction products.

1.1. Theoretical background

1.1.1. Simulating roller compaction

In order to manufacture representative ribbon samples, a means of simulating a roller compactor is necessary (Fig. 1). A mathematical expression based on a sine function is derived to model the movement of

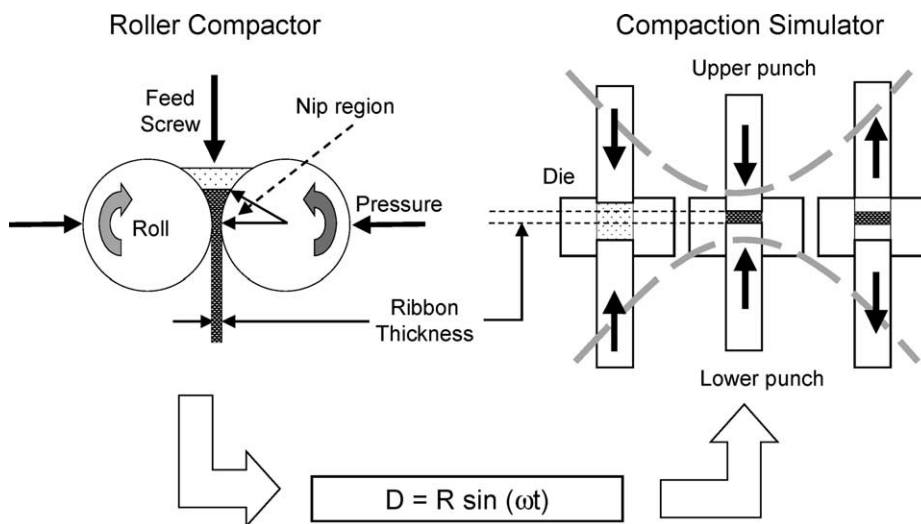


Fig. 1. Simulating a roller compactor using a compaction simulator (D is displacement, R is roll radius, ω is roll rotation frequency, t is time).

a tangential point on the circumference of the roller Eq. (1).

$$\text{Displacement} = R \sin(\omega t) \quad (1)$$

This model is used to control the upper and lower punch displacement profiles of the compaction simulator where R is the radius of each roller (mm), ω is the roller rotation rate (s^{-1}), and t is time (s). When $t = 0$, the punches begin their travel towards one another and compress the powder at the same strain rate as in the real roller compaction process. The “crest” of the sine wave correlates to the point at which the punches (or roller points) reach their minimum separation and can be used to target the thickness of the simulated ribbons. Once the punches reach their minimum separation, they retract to decompress the ribbon before it is ejected by the lower punch to the die surface.

This simulation utilizes a “batch” process to mimic a continuous one. As such, it does not account for roller compaction variables associated with continuous operation such as powder feed mechanisms, the nature of the shear forces experienced by the powder or the transition from the slip to no-slip region of compaction. For the simulation purposes, the contact of the upper punch with the powder during compression can be considered to simulate the onset of the no-slip region. Despite these factors, the simulation is considered as a representative tool for formation of ribbons since it enables control of the critical process variables such as roll separation, speed, pressure and radius.

To simulate the common roll surfaces of the roller compactor, two types of tooling are necessary. Rectangular, flat-faced, tooling can be used to mimic the surface of flat rollers, while the serrated rollers, commonly used as an aid for material flow into the compression (nip) region, can be mimicked by rectangular, serrated tooling. Measurement of the serrated roll surface morphology of a standard roll can provide dimensions for the design of such a tooling.

1.1.2. Material densification and key ribbon attributes

To show that roller compacted ribbons can be reproduced on the compaction simulator, appropriate ribbon quality indicators must be identified. Perhaps the most intuitive of these is material relative density or solid fraction. This parameter can be determined

from the following relationship:

$$\text{SF} = \frac{\rho_e}{\rho_t} = \frac{100 - P}{100} \quad (2)$$

where ρ_e is the envelope density of a sample, ρ_t is the true density of the material, P and SF are sample porosity and solid fraction, respectively.

Envelope density is defined as:

$$\rho_e = \frac{m}{V_e} \quad (3)$$

where V_e is the apparent volume of the object, including pores and small cavities, and m is the object mass.

Generally the solid fraction increases as the material is processed from powder to tablet form (Hancock et al., 2003) and is thus an indicator of the degree to which the powder has been compressed. The degree of densification in turn directly affects the mechanical properties of materials. Tensile strength, elastic modulus and indentation hardness of compacted powders, for instance, all depend on the solid fraction of the material (Davies and Newton, 1996; Rowe and Roberts, 1996). Mechanical properties consequently affect material behavior during processing.

Thus, provided that the unit operation process variables significantly affect the material solid fraction and this ribbon property can be reproducibly measured, solid fraction can be used as an indicator of product quality. This type of assessment is advantageous over product characterization using parameters such as compaction pressure or force because it relies on the inherent ribbon properties, and not gauge readings biased for each type of equipment, instrumentation and measurement method.

For ribbons, material densification is a function of multiple factors: powder properties such as flow, bulk and tapped density, processing parameters such as roll pressure and speed, as well as instrument geometry factors such as roll and feed screw size. This makes solid fraction an attractive attribute for evaluation of product quality as a function of the processing pathway. However, in situations where comparison of ribbon quality as a function of processing pathway and across material types is required, solid fraction alone is not sufficient for characterization of ribbon properties. This is due to the fact that despite equivalent densification, compaction of two different substances can result in compacts with different mechanical

characteristics. In such cases a suitable mechanical property should also be identified and monitored. Tensile fracture strength is defined as the minimum tensile stress required for fracture initiation within a compact (Hiestand, 2002) and is thus an indicator of bond strength within a specimen. This mechanical property has long been used in the industry as a gauge of tablet strength. As with tablets, it is expected that tensile fracture strength of ribbons can be indicative of their behavior during the subsequent processing steps. For example, one may expect to obtain equivalent granulations upon milling of ribbons with the same tensile strengths. Other properties (ductility, brittleness, etc.) affecting deformation and fragmentation of compacts will also be important. However, since the most critical physical characteristics of granules for their performance during processing are their size, solid fraction and mechanical strength (Alderborn, 1996), in this work the tensile fracture strength and solid fraction were considered the primary indicators of ribbon behavior during processing.

1.1.3. Experimental hypothesis

Based on the relationships discussed above, a hypothesis regarding the simulation of roller compaction is proposed: Two compacts, in this case ribbons, of the same material compressed to the same solid fraction should exhibit equivalent mechanical properties (tensile strengths). Thus, if ribbons of the same material and solid fraction are manufactured using both a real roller compactor and an accurate simulation of the roller compaction process, their mechanical properties should not exhibit significant differences, making the simulation feasible.

2. Experimental design, materials and methods

2.1. Experimental design

Two series of experiments were conducted to provide evidence for simulation validity:

- I. To determine the solid fraction range for the simulation study, the solid fraction of real roller compacted ribbons of various development formulations was measured.
- II. A model excipient, microcrystalline cellulose, was used to demonstrate equivalence between the real

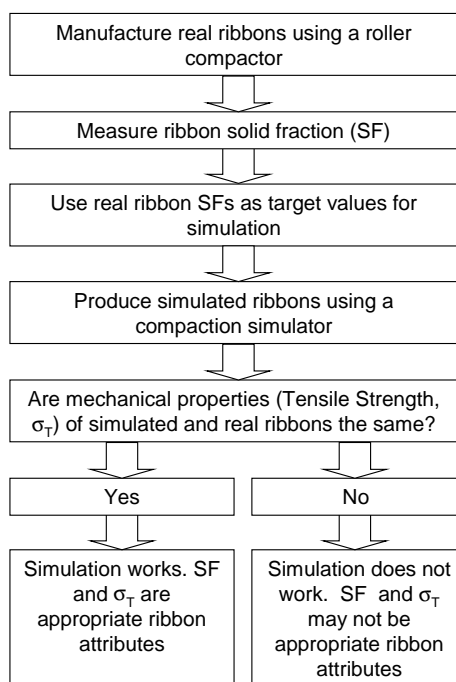


Fig. 2. Simulation of roller compaction process: proof of concept.

and simulated ribbons (Fig. 2). Real ribbons were produced using a roller compactor and their thickness and solid fractions were measured. These values were then used as target parameters for the manufacture of simulated ribbons using a compaction simulator. The tensile fracture strengths of both types of ribbons were then evaluated. Limiting conditions were set to provide a range of solid fraction and tensile strength values at which two ribbons can be considered equivalent. For the purposes of this study, ribbons, produced at the same solid fraction (± 0.02) were considered to exhibit equivalent mechanical properties if their tensile strength values fell within one standard deviation of each other.

2.2. Materials

Real ribbons produced from a range of placebo and active formulations were used in solid fraction analysis. These proprietary formulations, designated as A–J, contained USP/NF excipients typically used for immediate and controlled release tablets.

For the simulation experiments, microcrystalline cellulose (Avicel PH 101, FMC Corporation, Philadelphia, PA, USA) was selected as the model material due to its propensity to form compacts at a wide range of roll pressures and its widespread use in the development of solid dosage forms. The material was used as supplied by the manufacturer and was stored at ambient laboratory conditions of 22 ± 2 °C and $40 \pm 5\%$ RH.

2.3. True density measurements

The true densities of materials were determined using a helium pycnometer (UltraPycnometer[®], Quantachrome Corporation, Boynton Beach, FL, USA) following the manufacturer recommended procedures. All measurements were conducted at 22 ± 2 °C, $40 \pm 5\%$ RH and instrument calibration was performed using standard stainless steel spheres of known mass and volume.

2.4. Preparation of development ribbons for the solid fraction survey

TF-mini or TF-156 roller compactors (Vector Corporation, Marion, IA, USA) equipped with die-punch serrated (DPS) rollers were used to manufacture the ribbons for the solid fraction survey. Since these formulations were processed for development and clinical supply purposes and material throughput was an important consideration, the use of DPS rollers was required to improve the material flow rate into the compression region of the compactor. The roll speeds, pressures and auger feed conditions used were 2–4 rpm, 10–50 kg_f/cm² and 5–30 rpm, respectively. All of the samples analyzed were collected at steady state operating conditions.

2.5. Preparation of ribbons for simulation experiments

2.5.1. Real ribbons

A TF-mini roller compactor was used to produce the real microcrystalline cellulose ribbons. A roll speed of 4 rpm and increasing roll pressures (hydraulic cylinder gauge pressure) from 10 to 45 kg_f/cm² at 5 kg_f/cm² increments were used. The ribbon thickness was kept approximately constant at 2 mm (relative standard deviation (RSD) of 3%) by adjusting

the powder feed-auger speed. Ribbon samples for each operating condition were collected once the steady state was reached. Since material throughput was not a primary consideration in this case, and flat surface ribbons are preferred for accurate tensile strength analysis (Section 2.7), smooth die-punch (DP) rolls were used to compact the microcrystalline cellulose ribbons. Simulated ribbons (Section 2.5.2) were deemed more suitable for determination of the serrations' effect on ribbon mechanical properties, since the serrated compacts produced using the compaction simulator are expected to be more uniform compared to real ribbons. Based on the authors' experience, the serrations are better preserved on the surface of the simulated ribbons compared to real ribbons upon exit from the compaction region. In addition, the serration dimensions for a roll of a real roller compactor may vary, sometimes within a single roll, thus increasing serration dimension variability.

2.5.2. Simulated ribbons

A custom-built compaction simulator (Carlson et al., 1998) was used to generate the simulated ribbons. A sinusoidal compression profile simulating a roll radius of 50 mm and roll speed of 4 rpm was utilized to replicate the settings of the roller compactor used to produce real microcrystalline cellulose ribbons. The pressures used ranged from 17 to 61 MPa. To simulate smooth ribbons, rectangular, 10 mm × 22 mm flat-faced steel tooling was used. To investigate the effect the serrations on ribbon properties, a set of 10 mm × 22 mm rectangular, serrated steel tooling was used. The tooling was designed based on the serrated roll surface morphology (serration depth, width and frequency along the roll circumference) from a flat clay imprint of the roll measured by a NewView 5000TM white light interferometer (Zygo[®] Corporation, Middletown, CT, USA). The simulated ribbons were produced to a thickness (measured between serrations where necessary) of approximately 2 mm (RSD of 1%).

A single roll speed of 4 rpm was selected for evaluation of the simulation. The rationale behind this selection is two-fold: (1) 4 rpm is a commonly used roll speed during operation of the TF-mini type roller compactors; (2) successful simulation of the compression events during the roller compaction at one roll speed and size should enable simulation of com-

paction at other roll speeds and sizes provided that the compaction simulator is capable of following the designated velocity–displacement profile, a prerequisite satisfied by the use of a compaction simulator capable of high speed tablet press simulation (Carlson et al., 1998).

2.6. Measurement of solid fraction

2.6.1. Real ribbons

Ribbon solid fraction was determined using Eq. (2). True density measurements were described earlier (Section 2.3) and envelope density was obtained by measurement of sample mass and envelope volume. The sample mass was measured using an analytical balance (Mettler-Toledo Inc., Columbus, OH, USA) while the envelope volume was measured using the GeoPyc[®] 1360 Envelope Density Analyzer (Micromeritics Instrument Co., Norcross, GA, USA). This instrument allows for accurate envelope volume measurements of irregular objects by a method analogous to volume measurement by fluid displacement. It is facilitated through an assembly consisting of a sample chamber, a plunger and DryFlo[™] (a free-flowing, dry medium composed of graphite lubricated glass micro-spheres). Since this medium exhibits a wide particle size distribution it can conform to the contours of irregularly shaped surfaces, thus allowing

measurements of volumes for a variety of sample shapes. During the test, the volume of the medium is determined at a certain plunger consolidation pressure. A sample is then placed into the chamber with the medium and the volume determined again, using the same consolidation pressure, to obtain the sample volume by difference (volume of (sample and medium) – volume of medium = volume of sample). The volume occupancy within the chamber is determined by measurement of the piston displacement before and after (ΔD) sample insertion and using a chamber specific area conversion factor (K) (Fig. 3):

$$V = \Delta D \times K \quad (4)$$

Modest consolidation pressures are applied during measurements to facilitate medium conformation to the sample surface without inducing sample dimensional changes. In this study, a pressure of 0.1 MPa was used during all measurements.

The envelope density analyzer was calibrated using two sets of cylindrical wafers. The first set consisted of three acetal polymer (Delrin[®]) wafers of 20 and 2 mm in diameter and thickness, respectively and was conducted to determine method reproducibility. The second set was used to confirm that similar results are obtained when using pharmaceutical compacts. Cylindrical placebo wafers produced by flat-faced, one inch diameter tooling and an eccentric single station

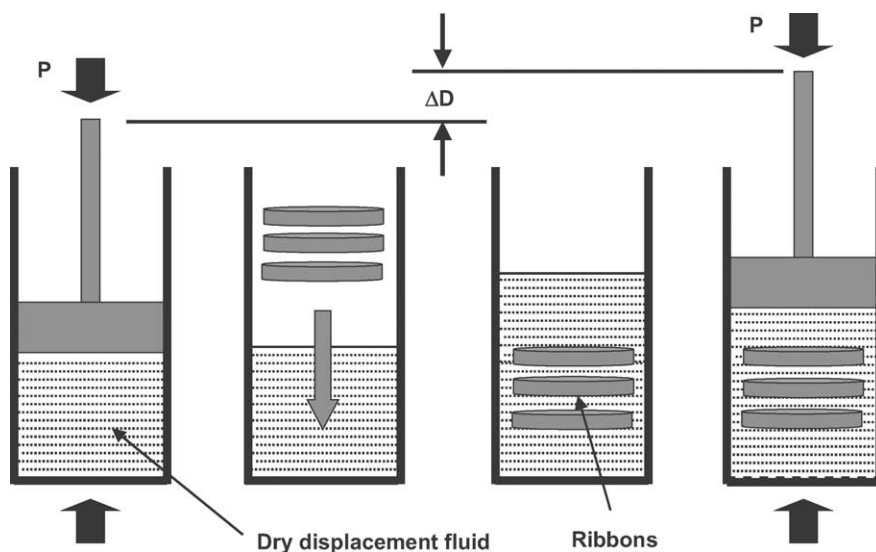


Fig. 3. Envelope density measurement method (P is consolidation pressure, ΔD is piston displacement).

tablet press (F-press, Manesty, Knowsley, Merseyside, UK) were used for this purpose and confirmed the reproducibility (RSD of 2.5%). The sample orientation and location along the depth of the chamber were kept constant to ensure that DryFlo™ packing densities remained uniform and consistent throughout the chamber and between wafers.

Samples for real ribbon solid fraction analysis were prepared by producing cylindrical wafers from the ribbons using a commercially available cork borer with inner diameter of 20 mm. The ribbon wafers were obtained from the center of the ribbon. Three wafers from random locations along the length of the ribbon produced at each roll pressure constituted a sample. The samples were equilibrated at $22 \pm 2^\circ\text{C}$, $40 \pm 5\%$ RH prior to measurement. Each ribbon sample was analyzed in triplicate. To compare the fluid displacement method results with a conventional method, the measurements of real ribbon sample volume were also carried out using traceable digital calipers (resolution: ± 0.005 mm).

2.6.2. Simulated ribbons

The envelope density of the simulated ribbons was determined through measurement of the sample mass and volume. The volume was determined from the sample dimensions (length, width and thickness), which were measured using traceable digital calipers. The solid fraction was subsequently determined by taking the ratio of ribbon envelope and true densities. Each measurement was conducted in triplicate and

samples were equilibrated at $22 \pm 2^\circ\text{C}$, $40 \pm 5\%$ RH prior to each measurement.

2.7. Measurement of ribbon tensile strength

The tensile strength of real and simulated ribbons was quantified using a three-point beam bending method. This technique is widely used in mechanical property testing of ceramic, polymeric and metallic materials (ASTM C1161, E1820, D790). Its applicability to evaluation of mechanical properties of pharmaceutical materials has also been demonstrated (Rowe and Roberts, 1996; Hancock et al., 2000). In this method, a rectangular sample is placed onto two supports separated by a known distance. A load is then applied to the middle of the top of the sample until the sample fails (Fig. 4). The tensile strength of the compact is determined from the following relationship:

$$\sigma_T = \frac{3 F \times S}{2 W \times t^2} \quad (5)$$

where σ_T is fracture tensile strength, F is the load applied at fracture, W is the width of sample, S is the distance between lower supports and t is the thickness of the sample. The above calculation applies provided that stress varies linearly across the compact thickness, from maximum tensile stress at the lower face of the beam, through zero to equivalent compressive stress on the upper surface of the beam. It is also assumed that linear elastic behavior occurs (Stanley, 2001).

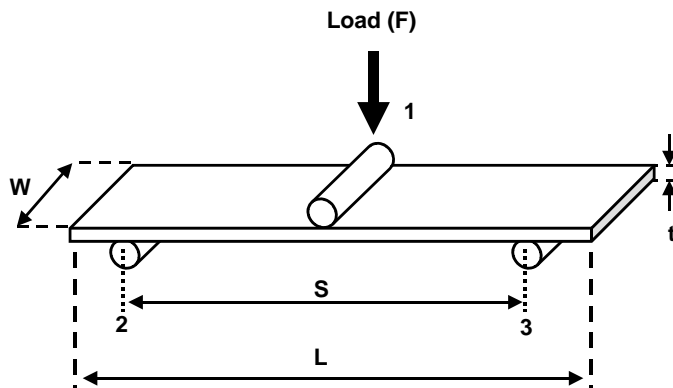


Fig. 4. Three point beam bending for tensile strength measurement (W , L and t are sample width, length and thickness, respectively, S is span, F is applied load; 1 is loading point, 2 and 3 are bottom supports).

A dynamic mechanical analyzer (DMA 2980, TA Instruments, Newcastle, DE, USA) was used for the three-point beam bending experiments. Appropriate instrument calibration, including force, position, electronics and clamp, using the manufacturer recommended procedures and standards was performed prior to ribbon evaluations. All of the samples were stored at controlled ambient conditions ($22 \pm 2^\circ\text{C}$, $40 \pm 5\%$ RH) for 48 h prior to testing. Initial investigations of the effects of loading rate on fracture strength of the samples showed that fracture strength values were relatively independent of this parameter. These findings are consistent with prior investigations involving microcrystalline cellulose (York et al., 1990; Rowe and Roberts, 1996). Thus, for the fracture strength evaluations ($n = 4$) a static load of 0.04 N was applied to each sample for 2 min followed by a 1.5 N/min load ramp until sample fracture. A three-point beam bending clamp ($S = 15$ mm) was used for fracture strength determinations. To facilitate the direct comparison between the tensile strengths of real and simulated ribbons, both types of samples were of the same dimensions. Real ribbon samples were prepared by cutting ribbons into 10 mm \times 22 mm (width \times length) compacts using a jeweler's precision table-saw (Preac Tool Co., North Bellmore, NY, USA) and simulated ribbons were produced as de-

scribed earlier. The thickness of both sample types was approximately 2 mm. The sample dimensions were primarily dictated by the geometry and loading capabilities of the dynamic mechanical analyzer and were comparable to dimensions previously used by Rowe and Roberts (1996).

3. Results and discussion

3.1. Solid fraction and material processing relationships

Table 1 lists the solid fraction ranges for real ribbons of ten different formulations measured using the fluid displacement and dimensional techniques. These formulations resulted in tablets with robust mechanical properties, indicating that the ribbons used to produce them were in turn of acceptable quality. The ribbon solid fraction for these materials ranged from 0.64 to 0.79 with a mean of 0.71 when measured using the envelope density analyzer and from 0.57 to 0.80 with a mean of 0.70 when measured using the calipers. The measurement of solid fraction using the envelope density analyzer showed less variability (mean RSD of 1.4%) than the caliper method (mean RSD of 4.6%). The greater variability

Table 1
Solid fraction of roller compacted ribbons for a range of development and clinical formulations

Formulation	Mean ribbon thickness (mm)	Solid fraction			
		Fluid displacement method		Caliper method	
		Mean	RSD ^a (%)	Mean	RSD (%)
A	1.82	0.715	1.8	0.715	1.3
B	1.75	0.749	2.4	0.788	0.5
C	1.66	0.785	2.4	–	–
D	1.40	0.679	2.3	0.678	2.5
E	1.80	0.644	1.0	0.572	13.6
F	1.99	0.686	1.2	0.632	6.6
G	1.80	0.677	0.9	0.683	5.2
H	1.40	0.688	1.4	–	–
I	1.70	0.713	0.5	0.798	6.1
J	2.20	0.755	0.5	0.686	0.6
Mean	1.75	0.709	–	0.694	–
Maximum	2.20	0.785	–	0.798	–
Minimum	1.40	0.644	–	0.572	–

^a RSD is relative standard deviation.

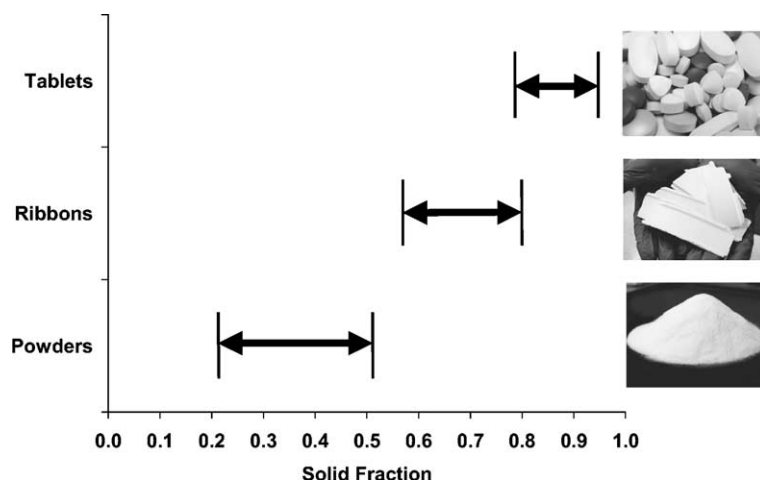


Fig. 5. Normal ranges for solid fraction of pharmaceutical materials: from powders to tablets.

of the caliper method can be explained by the fact that the envelope volume determinations using this technique assume a perfectly rectangular sample geometry, and in reality, roller compacted ribbons, exhibit relatively rough and uneven edges. The envelope density technique avoids such volume measurement error since the fluid media should conform to the surface of samples with irregular geometries and dimensions.

To identify the location of roller compacted ribbons on the solid fraction spectrum, this parameter was also obtained for materials in powder and tablet form. Fig. 5 shows the relationship between the stages of powder processing and the material solid fraction based on the data measured here and previously reported by Hancock et al. (2003). The powdered materials exhibited the lowest solid fraction values and the broadest range (0.21–0.57). In contrast, tableted materials occupied the highest end of the solid fraction spectrum with a narrow solid fraction distribution (0.77–0.93). As evident by the ranges of values obtained for the powders, ribbons and tablets, the solid fraction is affected by the nature of the materials and the unit operation parameters used to process them. The solid fraction ranges for various product types (i.e., tablets versus ribbons), however, are rather discrete and thus allow one to target a particular solid fraction to obtain an acceptable product (i.e., 0.6–0.8 for ribbons).

3.2. Solid fraction—compaction pressure relationships for microcrystalline cellulose

Fig. 6 illustrates the relationship between roller compaction pressure and solid fraction of the real microcrystalline cellulose ribbons as measured by two methods, the fluid displacement technique and standard calipers. The increase in ribbon solid fraction as a function of roll pressure was approximately linear for solid fractions of up to 0.75. It has been widely reported that the relative density versus pressure relationship for microcrystalline cellulose does not follow linear behavior (Sonnergaard, 1999; Hancock et al., 2001). However, the data indicating non-linearity has been obtained at significantly higher solid fraction ranges than those reported in this publication. It is expected that deviation from linearity would have been observed if the real ribbons had been compressed to higher (0.8–0.9) solid fractions.

A similar increase of solid fraction with compression pressure was observed for the simulated ribbons (data not shown) suggesting that analogous compression events occurred during the simulation. For simulated ribbons, two sets of compacts were manufactured at higher solid fractions (0.78 and 0.82) than the maximum solid fraction of real ribbons. The inclusion of these points in the solid fraction and pressure relation for microcrystalline cellulose shows the

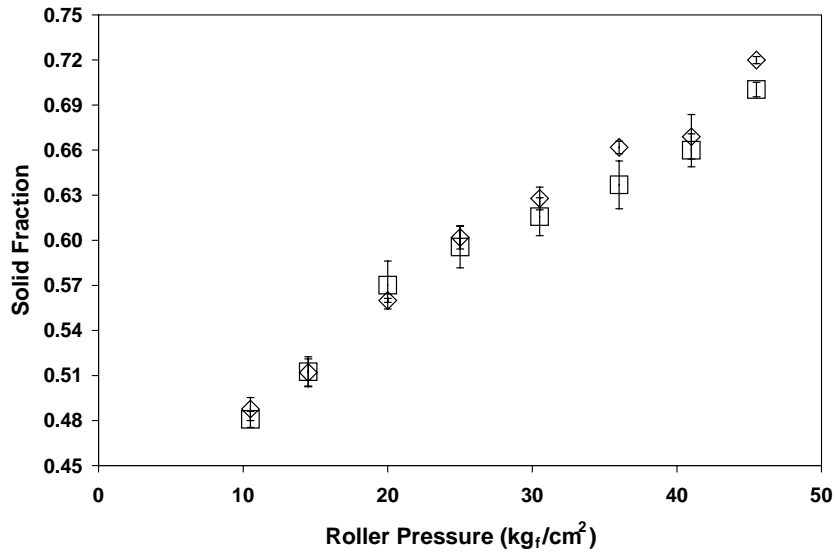


Fig. 6. Solid fraction of real ribbons as a function of roller pressure as measured by the envelope density analyzer (◇) and caliper (□) techniques (error bars are standard deviations for each measurement).

onset of commonly observed non-linear compression behavior. The estimated yield pressure of microcrystalline cellulose, obtained from zero pressure Heckel plots using simulated ribbons, was 82 MPa. This value is in agreement with previously published yield pressures of same-grade microcrystalline cellulose determined using various instruments, stress

conditions and solid fraction measurement techniques (48–104 MPa) (Sonnergaard, 1999).

3.3. Evaluation of the roller compaction simulation

The tensile strengths of simulated and real ribbons are shown in Fig. 7. The tensile fracture strengths

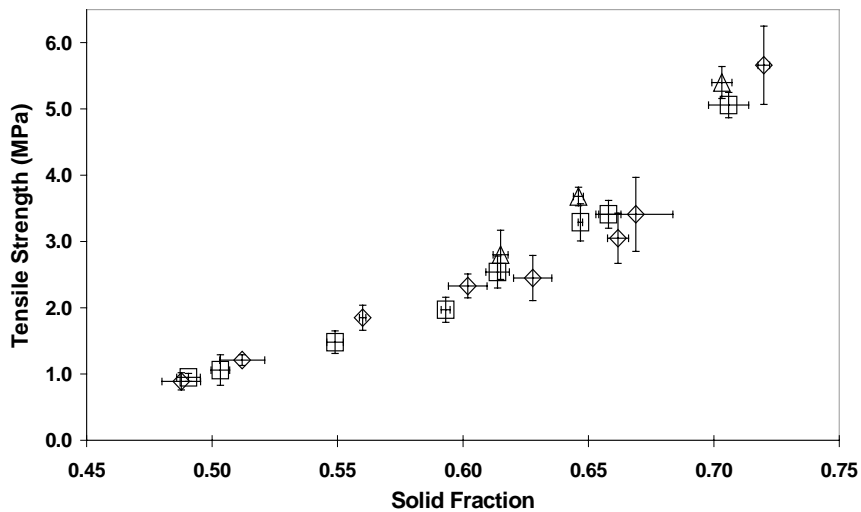


Fig. 7. Tensile strength comparison of real and simulated ribbons as a function of solid fraction (real ribbons (smooth) (◇), simulated ribbons (smooth) (□), simulated ribbons (serrated) (△), error bars are standard deviations for each measurement).

of both ribbon types followed an exponential increase with solid fraction (linear regression analysis $R^2 = 0.96$ and $R^2 = 0.98$ for simulated and real ribbons, respectively). These findings are consistent with the strength and porosity relationships for microcrystalline cellulose reported by other authors (Mashadi and Newton, 1987; Roberts et al., 1995) despite the somewhat higher solid fraction values utilized in those studies.

Variability of solid fraction and tensile strength data depicted in Fig. 7 also provides insight into the character of both types of ribbons and into the nature of the simulation. Larger standard deviations of tensile strength measurements were observed for ribbons produced at higher compaction pressures. This variation may be an indicator of micro-cracks within the specimens induced under these conditions. It was also observed that the real ribbons exhibited non-uniform stress distributions across their length and width resulting in higher variability of thickness and solid fraction. Such behavior is not uncommon to roller compacted materials and has been reported by other authors (Simon and Guigon, 2003). Overall, the real ribbons exhibited a higher variability in tensile strength and solid fraction than the simulated ribbons. The compaction simulator is capable of generating ribbons with very consistent and uniform properties and in some senses the simulation of the roller compaction process using such an instrument may be “too good.”

Fig. 7 shows that the tensile strengths of real and simulated ribbons of similar solid fractions were equivalent (within one standard deviation of each other). Although some differences exist between the simulation results obtained by measurement of real ribbon solid fractions using the fluid displacement technique and calipers, such differences were deemed insignificant when variability in the measurement of the ribbon attributes was taken into consideration. The equivalent ribbon tensile strengths also show that the shear forces experienced by the material during real roller compaction (an aspect of roller compaction not simulated using a compaction simulator) should not have a significant effect on ribbon mechanical properties relevant to further ribbon processing. Fig. 7 also shows that serrations made a minimal contribution to the fracture strength of ribbons. The slight tensile strength differences observed between serrated and smooth ribbons could be attributed to a small

increase in effective thickness of the serrated ribbons compared to the smooth ribbons. In addition, it is important to point out that Eq. (5) (used to determine the sample tensile strength) applies strictly to a rectangular, flat specimen. Thus, its application to the serrated specimens results only in an estimate of their tensile strengths.

Overall, the mechanical and physical properties of real and simulated ribbons are equivalent when normal variations in the solid fraction and tensile strength determinations are considered. Processing of both types of ribbons is thus expected to result in equivalent granulations. Although, the simulation clearly enables valid reproduction of roller compaction products, it is important to remark that certain features of roller compaction, such as non-homogeneous ribbon density, material feeding patterns and bypass, cannot be mimicked using the compaction simulator. These aspects are important and should be compensated for each individual formulation (e.g., addition of a designated amount of un-compacted powder into the granulation to simulate material bypass). Despite these factors, the simulation provides marked advantages to the current roller compaction development practices.

3.4. Application to roller compaction development methods

The simulation and key ribbon property approach described in this paper can be used for process specific predictive and scale up studies while significantly reducing material requirements. The simulation requires only a fraction of material to conduct roller compaction feasibility studies compared to conventional roller compaction equipment ($\sim 10\times$ reduction). Also, unlike the tablet press slugging experiments, the simulation enables more relevant feasibility studies by addressing the effects of roller compaction specific process variables such as roll pressure, speed and size on ribbon properties. The results obtained from such studies can be readily scaled up on the basis of ribbon manufacture at equivalent solid fraction and/or tensile fracture strength (due to non-homogeneity along the width and length of the ribbon, attention should be paid to the sampling location during the scale-up studies, where sampling at different locations may result in inconsistent product performance). An empirical correlation analogous to the one shown in Fig. 8, can

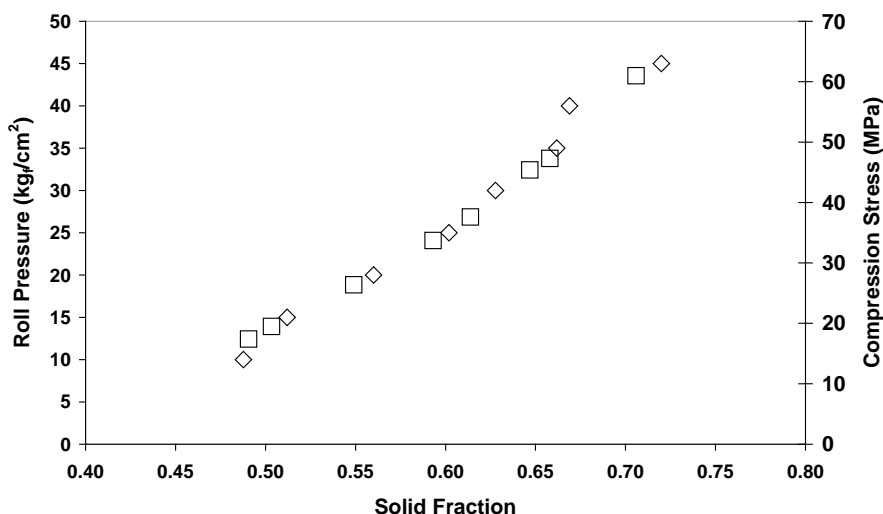


Fig. 8. Comparison of roller pressure and compression stress for roller compactor and compaction simulator (real ribbons (□), simulated ribbons (◇)).

be obtained for a number of instrument and material combinations to enable the scale up between the compaction simulator and the roller compactor. This scaling is based on the most relevant component of the manufacturing process: consistent product properties, and is independent of measured parameters such as hydraulic cylinder/roll pressure. The simulation and constant ribbon property approach, allows for de-convolution of ribbon quality from instrument parameters, and should result in consistent process scale-up or transfer between instrument types.

4. Conclusions

A method for simulation of the roller compaction process was developed. This was achieved by mimicking the compression events that occur during roller compaction using a compaction simulator. Solid fraction and tensile strength were identified as key indicators of ribbon quality and were used in evaluation of the simulation. It was shown that real and simulated microcrystalline cellulose ribbons of the same solid fraction exhibited equivalent mechanical properties (tensile strengths) and are thus expected to result in equivalent granulations. The improved material efficiency of the simulation and consistent product scale-up methods, based on equivalent ribbon

properties, could enable formulation of tablet dosage forms earlier in the drug development process.

Acknowledgements

Cindy Oksanen, Dan Arenson, Dauda Ladipo, Tim McDermott and members of the Pfizer Inc., Groton solid dosage form clinical manufacturing facility are greatly thanked for their contributions to this work.

References

- Adeyeye, M.C., 2000. Roller compaction and milling pharmaceutical unit processes: part I. *Am. Pharm. Rev.* 3, 37–42.
- Aldern, G. 1996. Granule properties. In: Aldern, G., Nystrom, C. (Eds.), *Pharmaceutical Powder Compaction Technology*, vol. 71. Marcel Dekker IN., New York, pp. 245–282.
- American Society for Testing and Materials (ASTM), 2001a. Standard test methods for flexural properties of unreinforced and reinforced plastics and electrical insulating materials, Standard D 79. pp. 1–9.
- American Society for Testing and Materials (ASTM), 2001b. Standard test method for measurement of fracture toughness, Standard E 1820-01, pp. 1–46.
- American Society for Testing and Materials (ASTM), 2002. Standard test method for flexural strength of advanced ceramics at ambient temperature, Standard C 1161-02a, pp. 1–16.

- Bateman, S.D., Rubinstein, M.H., Rowe, R.C., Roberts, R.J., Drew, P., Ho, A.Y.K., 1989. A comparative investigation of compression simulators. *Int. J. Pharm.* 49, 209–212.
- Britten, J.R., Barnett, M.I., Armstrong, N.A., 1996. Studies on powder plug formation using a simulated capsule filling machine. *J. Pharm. Pharmacol.* 48, 249–254.
- Carlson, G.T., Christie, H.R.C., Curtiss, A.C., Hausberger, A.G., Jarvas, R.E., Jaxheimer, B.J., Schelhorn, J.S., Sinko, C.M., 1998. Design, fabrication and startup of a laboratory scale compaction simulator. In: Proceedings of the AAPS Annual Meeting, San Francisco, CA.
- Celik, M., Marshall, K., 1989. Use of a compaction simulator system in tableting research. *Drug. Dev. Ind. Pharm.* 15, 759–800.
- Davies, N.P., Newton, M.J. 1996. Mechanical strength. In: Alderborn, G., Nystrom, C. (Eds.), *Pharmaceutical Powder Compaction Technology*, vol. 71. Marcel Dekker, New York, pp. 165–192.
- Falzone, A.M., Peck, G.E., McCabe, G.B., 1992. Effects of changes in roller compactor parameters on granulations produced by compaction. *Drug. Dev. Ind. Pharm.* 18, 469–489.
- Gereg, G.W., Cappola, M.L., 2002. Roller compaction feasibility for new drug candidates. *Pharmaceutical Technology Yearbook*. pp. 14–23.
- Hancock, B.C., Colvin, J.T., Mullarney, M.P., Zinchuk, A.V., 2003. The relative density of pharmaceutical powders, blends, dry granulations and immediate release tablets. *Pharmaceutical Technology*. April, pp. 64–80.
- Hancock, B.C., Christensen, K., Clas, S.-D., 2000. Micro-scale measurement of the mechanical properties of compressed pharmaceutical powders. I. The elasticity and fracture behavior of microcrystalline cellulose. *Int. J. Pharm.* 209, 27–35.
- Hancock, B.C., Dalton, C.R., Clas, S.-D., 2001. Micro-scale measurement of the mechanical properties of compressed pharmaceutical powders. II. The dynamic moduli of microcrystalline cellulose. *Int. J. Pharm.* 228, 139–145.
- Heda, P.K., Muller, F.X., Augsburger, L.L., 1999. Capsule filling machine simulation. I. Low-force powder compression physics relevant to plug formation. *Pharm. Dev. Tech.* 4, 209–219.
- Hiestand, E.N., 2002. Mechanics and physical principles for powders and compacts. *Foundations of Pharmaceutical Sciences Series*, 2nd ed. SSCI Inc., West Lafayette, IN.
- Inghelbrecht, S., Remon, J.P., 1998. The roller compaction of different types of lactose. *Int. J. Pharm.* 166, 135–144.
- Johanson, J.R., 1965. A rolling theory for granular solids. *J. Appl. Mech.* 32, 842–848.
- Johanson, J.R., 1973. Predicting limiting roll speeds for briquetting presses. *Proc. 13th Biennial Conf. Inst. Briquetting Agglomerat.* 13, 89–99.
- Jolliffe, I.G., Newton, J.M., Cooper, D., 1982. The design and use of an instrumented mG2 capsule filling machine simulator. *J. Pharm. Pharmacol.* 34, 230–235.
- Mashadi, A.B., Newton, J.M., 1987. The characterization of the mechanical properties of microcrystalline cellulose: a fracture mechanics approach. *J. Pharm. Pharmacol.* 37, 961–965.
- Miller, R.W., 1997. Roller compaction technology. In: Parikh, D.M. (Ed.), *Handbook of Pharmaceutical Granulation Technology*. Marcel Dekker, New York, pp. 99–149.
- Murray, M., Laohavichien, A., Habib, W., Sakr, A., 1998. Effect of process variables on roller-compacted ibuprofen tablets. *Pharm. Ind.* 60, 257–262.
- Roberts, R.J., Rowe, R.C., York, P., 1995. The relationship between the fracture properties, tensile strength and critical stress intensity factor of organic solids and their molecular structure. *Int. J. Pharm.* 125, 157–162.
- Rowe, R.C., Roberts, R.J., 1996. Mechanical properties. In: Alderborn, G., Nystrom, C. (Eds.), *Pharmaceutical Powder Compaction Technology*, vol. 71. Marcel Dekker, New York, pp. 283–322.
- Sheskey, P.J., Cabelka, T.D., Robb, R.T., Boyce, B.M., 1994. Use of roller compaction in the preparation of controlled-release hydrophilic matrix tablets containing methylcellulose and hydroxypropyl methyl cellulose polymers. *Pharm. Tech.* 18, 132–140.
- Simon, O., Guigon, P., 2003. Correlation between powder-packing properties and roll press compact heterogeneity. *Powder Technol.* 130, 257–264.
- Sonnergaard, J.J., 1999. A critical evaluation of Heckel equation. *Int. J. Pharm.* 193, 63–71.
- Stanley, P., 2001. Mechanical strength testing of compacted powders. *Int. J. Pharm.* 227, 27–38.
- York, P., Bassam, F., Rowe, R.C., Roberts, R.J., 1990. Fracture mechanics of microcrystalline cellulose powders. *Int. J. Pharm.* 66, 143–148.